20) Lowenfels, A. B., Lindström, C. G., Conway, M. J. and Hastings, P. R. : Gallstones and risk of gallbladder cancer. J. Natl. Cancer Inst., 75 : 77～80, 1985.
21) Nervi, F., Duarte, I., Gómez, G., Rodríguez, G., Del Pino, G., Ferrerio, O., Covarrubias, C., Valdivieso, V., Torres, M. I. and Urzúa, A. : Frequency of gallbladder cancer in Chile, a high-risk area. Int. J. Cancer, 41 : 657～660, 1988.
22) Combined oral contraceptives and gallbladder cancer : The WHO Collaborative Study of Neoplasia and Steroid Contraceptives. Int. J. Epidemiol., 18 : 309～314, 1989.
23) Kato, K., Akai, S., Tominaga, S. and Kato, I. : A case-control study of biliary tract cancer in Niigata Prefecture, Japan. Jpn. J. Cancer Res., 80 : 932～938, 1989.
24) Zatonski, W. A., Lowenfels, A. B., Boyle, P., Maisonneuve, P., Bueno de Mesquita, H. B., Ghadirian, P., Jain, M., Przewozniak, K., Baghurst, P., Moerman, C. J., Simard, A., Howe, G. R., McMichael, A. J., Hsieh, C. C. and Walker, A. M. : Epidemiologic aspects of gallbladder cancer : A case-control study of the SEARCH Program of the International Agency for Research on Cancer. J. Natl. Cancer Inst., 89 : 1132～1138, 1997.
25) Okamoto, M., Okamoto, H., Kitahara, F., Kobayashi, K., Karikome, K., Miura, K., Matsumoto, Y. and Fujino, M. A. : Ultrasonographic evidence of association of polyps and stones with gallbladder cancer. Am. J. Gastroenterol., 94 : 446～450, 1999.
26) Khan, Z. R., Neugut, A. I., Ahsan, H. and Chabot, J. A. : Risk factors for biliary tract cancers. Am. J. Gastroenterol., 94 : 149～152, 1999.
27) 伊佐山浩通：胆石があると胆嚢癌になりやすいか？ 跡見裕，上村直実，白鳥敬子，正木尚彦編，臨床に直結する肝・胆・膵疾患治療のエビデンス，文光堂，東京，2007，p. 177～178.
28) Ishiguro, S., Inoue, M., Kurahashi, N., Iwasaki, M., Sasazuki, S. and Tsuqane, S. : Risk factors of biliary tract cancer in a large-scale population-based cohort study in Japan (JPHC study) ; with special focus on cholelithiasis, body mass index, and their effect modification. Cancer Causes Control, 19 : 33～41, 2008.
29) 胆道癌診療ガイドライン作成出版委員会編：エビデンスに基づいた胆道癌診療ガイドライン，医学図書出版，東京，2007.
30) Fendrick, A. M., Gleeson, S. P., Cabana, M. D. and Schwartz, J. S. : Asymptomatic gallstones revisited. Is there a role for laparoscopic cholecystectomy? Arch. Fam. Med., 2 : 959～968, 1993.

Novel Function of Niemann-Pick C1-Like 1 as a Negative Regulator of Niemann-Pick C2 Protein

AQ1 Yoshihide Yamanashi,[1,2] Tappei Takada,[1] Jun-Ichi Shoda,[3] and Hiroshi Suzuki[1]

The hepatic expression of Niemann-Pick C1-like 1 (NPC1L1), which is a key molecule in intestinal cholesterol absorption, is high in humans. In addition to NPC1L1, Niemann-Pick C2 (NPC2), a secretory cholesterol-binding protein involved in intracellular cholesterol trafficking and the stimulation of biliary cholesterol secretion, is also expressed in the liver. In this study, we examined the molecular interaction and functional association between NPC1L1 and NPC2. *In vitro* studies with adenovirus-based or plasmid-mediated gene transfer systems revealed that NPC1L1 negatively regulated the protein expression and secretion of NPC2 without affecting the level of NPC2 messenger RNA. Experiments with small interfering RNA against NPC1L1 confirmed the endogenous association of these proteins. In addition, endocytosed NPC2 could compensate for the reduction of NPC2 in NPC1L1-overexpressing cells, and this demonstrated that the posttranscriptional regulation of NPC2 was dependent on a novel ability of NPC1L1 to inhibit the maturation NPC2 and accelerate the degradation of NPC2 during its maturation. Furthermore, to confirm the physiological relevance of NPC1L1-mediated regulation, we analyzed human liver specimens and found a negative correlation between the protein levels of hepatic NPC1L1 and hepatic NPC2. *Conclusion*: NPC1L1 down-regulates the expression and secretion of NPC2 by inhibiting its maturation and accelerating its degradation. NPC2 functions as a regulator of intracellular cholesterol trafficking and biliary cholesterol secretion; therefore, in addition to its role in cholesterol re-uptake from the bile by hepatocytes, hepatic NPC1L1 may control cholesterol homeostasis via the down-regulation of NPC2. (HEPATOLOGY 2011;00:000–000)

Niemann-Pick C1-like 1 (NPC1L1) is a key protein involved in intestinal cholesterol absorption.[1,2] In most animal species, NPC1L1 is highly expressed in the proximal intestine (where dietary cholesterol is absorbed).[1,3-5] In humans, it has been reported that NPC1L1 is highly expressed in the liver, in addition to the intestine.[1,3] *In vivo* studies of mice expressing human NPC1L1 from a liver-specific promoter have revealed that hepatic NPC1L1 may be involved in cholesterol reabsorption from the bile by hepatocytes.[6] On the basis of these findings, NPC1L1 is believed to play critical roles in cholesterol uptake in the intestine and in re-uptake in the liver.

Abbreviations: ABC, adenosine triphosphate–binding cassette; Ad-GFP, green fluorescent protein–expressing adenovirus; Ad-NPC1L1, Niemann-Pick C1-like 1–expressing adenovirus; Ad-NPC1L1-HA, Niemann-Pick C1-like 1/HA–expressing adenovirus; Ad-NPC2-Myc-His, Niemann-Pick C2/Myc-His–expressing adenovirus; CHO-K1, Chinese hamster ovary K1; Endo H, endoglycosidase H; ER, endoplasmic reticulum; GM2AP, GM2 ganglioside activator protein; HMW, higher molecular weight; IB, immunoblot; IP, immunoprecipitate; LMW, lower molecular weight; LXR, liver X receptor; MG132, N-(benzyloxycarbonyl)leucinylleucinylleucinal; MOI, multiplicity of infection; mRNA, messenger RNA; NgBR, Nogo-B receptor; NPC, Niemann-Pick C; NPC1L1, Niemann-Pick C1-like 1; NS, not significant; PCR, polymerase chain reaction; PNGase F, peptide N-glycosidase F; R_s, Spearman's rank correlation coefficient; AQ2 *siControl, control small interfering RNA; siNPC1L1, small interfering RNA targeted against Niemann-Pick C1-like 1; WT, wild type.*

From the Departments of [1]Pharmacy and [2]Pharmacology and Pharmacokinetics, University of Tokyo Hospital, Faculty of Medicine, University of Tokyo, Tokyo, Japan; and [3]Division of Sports Medicine, Graduate School of Comprehensive Human Sciences, Tsukuba University, Ibaraki, Japan.

Received May 20, 2011; accepted October 8, 2011.

This work was supported by grants from the Japanese Ministry of Education, Culture, Sports, Science, and Technology and by a Grant-in-Aid for Scientific AQ3 *Research on Innovative Areas for the High-Definition Physiology project (22136015).*

Address reprint requests to: Tappei Takada, Ph.D., Department of Pharmacy, University of Tokyo Hospital, Faculty of Medicine, University of Tokyo, 7-3-1 Hongo, Bunkyo-Ku, Tokyo, Japan 113-8655. E-mail: tappei-tky@umin.ac.jp; fax: +81-3-3816-6159.

View this article online at wileyonlinelibrary.com.

DOI 10.1002/hep.24772

Potential conflict of interest: Nothing to report.

Additional Supporting Information may be found in the online version of this article.

NPC1L1 was originally identified as a homolog of Niemann-Pick C1 (NPC1)[7]; mutations of the latter result in the acquisition of NPC disease, which is a neurovisceral disorder characterized by an accumulation of free cholesterol within endosomes and lysosomes.[8,9] In addition to mutations in the NPC1 gene, mutations in the NPC2 gene also cause an accumulation of cholesterol in late endosomes and lysosomes and can result in the development of NPC disease in some patients.[10] NPC2 is a small secretory protein that is widely expressed in the body and specifically binds unesterified sterols with nanomolar affinity.[11] Recent studies have revealed that NPC2 can transfer its bound cholesterol to NPC1 in late endosomes and lysosomes to facilitate intracellular cholesterol trafficking.[12,13]

In addition to its role as a regulator of intracellular cholesterol trafficking, NPC2 may contribute to whole-body cholesterol homeostasis. Klein et al.[14] found that NPC2 is expressed in the liver and secreted into the bile in both mice and humans. Moreover, in a recent study,[15] we found that biliary NPC2 positively regulates biliary cholesterol secretion by stimulating cholesterol efflux, which is mediated by a heterodimer of adenosine triphosphate–binding cassette G5 (ABCG5) and ABCG8, a cholesterol exporter expressed in the liver.[16] Physiologically, the amount of cholesterol secreted into the bile each day is similar to the amounts synthesized in the liver and absorbed from the intestine,[17] and this suggests the importance of biliary cholesterol in cholesterol homeostasis. The biliary secretion of NPC2 is, therefore, thought to be important in the maintenance of the whole-body cholesterol level.

Although it has been shown that NPC2 cooperates with NPC1[12,13] and ABCG5/ABCG8,[15] the functional interaction between NPC1L1 and NPC2 has not yet been clarified. Although it has been demonstrated that secreted NPC2 has little effect on NPC1L1-mediated cholesterol uptake,[15,18] considering the fact that NPC1L1 is expressed in intracellular compartments besides the plasma membrane,[3] we have hypothesized that there may be an intracellular interaction between NPC1L1 and NPC2.

In this article, we show that NPC1L1 interacts with NPC2 during the maturation of NPC2. In addition, the results of *in vitro* assays with NPC1L1-overexpressing cells or cells in which NPC1L1 was knocked down with small interfering RNA as well as analyses with human liver specimens indicate that NPC1L1 downregulates the protein expression and secretion of NPC2 by inhibiting its maturation and by accelerating its degradation during the maturation process. These findings demonstrate a novel function of NPC1L1 as a negative regulator of NPC2 in addition to its role as a cholesterol (re-)uptake transporter.

Materials and Methods

Construction of Expression Vectors and Recombinant Adenoviruses. The human NPC1L1-HA vector was constructed as reported previously.[2,19,20] The human NPC2-Myc-His vector and the human GM2 ganglioside activator protein (GM2AP)–Myc–His vector were constructed as described in the supporting information.

Recombinant adenoviruses expressing each complementary DNA [Niemann-Pick C1-like 1–expressing adenovirus (Ad-NPC1L1), Niemann-Pick C1-like 1/HA–expressing adenovirus (Ad-NPC1L1-HA), and Niemann-Pick C2/Myc-His–expressing adenovirus (Ad-NPC2-Myc-His)] were prepared with the Adeno-X Tet-Off 1 expressing system (Takara Bio, Inc., Shiga, Japan) according to the manufacturer's instructions and were purified by cesium chloride gradient centrifugation. A tetracycline-responsive transcriptional activator–expressing adenovirus and a green fluorescent protein–expressing adenovirus (Ad-GFP)[21] were purified with the same method. The titer of each purified virus (plaque-forming units per milliliter) was determined with the Adeno-X rapid titer kit (Takara Bio), and the multiplicity of infection (MOI) was determined by the normalization of the virus titer to the cell count in each experiment.

Immunoblot Analyses. Immunoblot analyses were performed as described in the supporting information.

Metabolic Labeling of NPC2. Chinese hamster ovary K1 (CHO-K1) cells infected with the indicated adenoviruses were first incubated in methionine/cysteine-free minimal essential medium (Invitrogen Life Technologies, Carlsbad, CA) for 30 minutes. The cells were then incubated in a labeling medium containing a 100 mCi/mL [^{35}S]methionine/cysteine cell labeling mix (PerkinElmer, Waltham, MA) and were collected at the indicated times. The cells were lysed with a radio immunoprecipitation assay buffer (0.1% sodium dodecyl sulfate, 0.5% deoxycholate, and 1% Nonidet P-40) and immunoprecipitated with 1 μg of a mouse anti-Myc antibody (Roche Applied Science, Indianapolis, IN), as described in the supporting information. The immunoprecipitates were separated by sodium dodecyl sulfate–polyacrylamide gel electrophoresis and exposed to a super-resolution phosphor imager

J_ID: ZHE Customer A_ID: 11-0942.R1 Customer Art: ZHE24772 Date: 5-November-11 Stage: Page: 3

(PerkinElmer). The radioactivity was detected with a Cyclone phosphor imager (Packard, Haverhill, MA).

Quantitative Real-Time Polymerase Chain Reaction (PCR). To determine the messenger RNA (mRNA) levels of NPC2 and NPC1L1, quantitative real-time PCR was performed as described in the supporting information.

Immunohistochemical Staining. Immunohistochemical staining with HepG2 cells was performed as described in the supporting information.

Cholesterol Staining. For the detection of free intracellular cholesterol, cells were fixed with 4% paraformaldehyde and stained with filipin according to the manufacturer's instructions (Cayman Chemicals). The relative intensity of filipin staining in intracellular compartments was quantified by the division of the intensity above the low threshold by the number of total pixels.[22,23]

Collection of Human Liver Specimens. All experiments involving human specimens were conducted according to a study protocol approved by the institutional review board of the University of Tokyo and Tsukuba University after informed consent was obtained from all subjects. Tumor tissue and surrounding tissue appearing to be grossly normal were obtained from nine liver cancer patients upon surgical resection. The tumor-adjacent normal tissue specimens were used for immunoblot analyses to determine the protein levels of NPC1L1 and NPC2 and for quantitative real-time PCR to determine the mRNA levels of these genes.

Results

NPC2 Coimmunoprecipitates With NPC1L1. To examine the interaction between NPC1L1 and NPC2, we performed a coimmunoprecipitation assay. As shown in Fig. 1, NPC2 in the total cell lysate was detected at approximately 20 to 26 kDa, as reported previously.[24] The lower molecular weight (LMW) form of NPC2 (20 kDa) coimmunoprecipitated with NPC1L1 (HA, Fig. 1). Conversely, NPC1L1 coimmunoprecipitated with NPC2 (Myc, Fig. 1). These results suggest that NPC1L1 can interact with LMW NPC2.

NPC1L1 Down-Regulates the Protein Expression of NPC2. The expression of NPC2 and particularly its higher molecular weight (HMW) forms, which are detected at approximately 26 kDa,[24] was markedly reduced by the coexpression of NPC1L1 in adenovirus-based experiments (input, Fig. 1). This reduction in the NPC2 protein level was also observed in plasmid-based experiments (lanes 2 and 3, Fig. 2A),

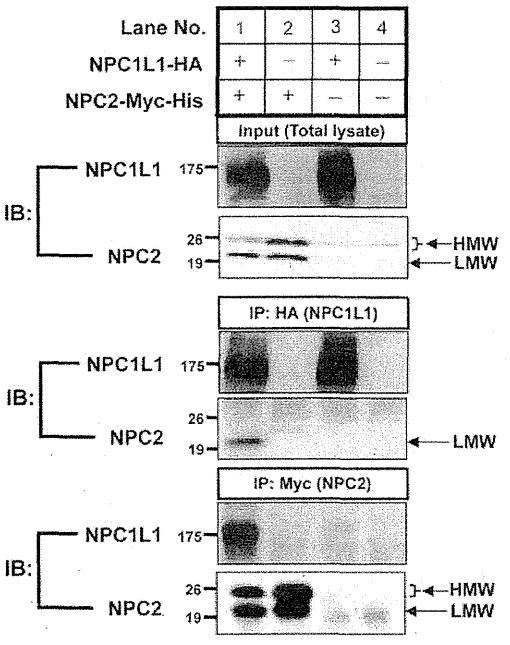

Fig. 1. Molecular association between NPC1L1 and NPC2. CHO-K1 cells were infected with Ad-NPC2-Myc-His, Ad-NPC1L1-HA, and Ad-GFP (the control) at 5 MOI. Twenty-four hours after infection, the cells were harvested, and a coimmunoprecipitation assay was performed as described in the supporting information. Anti-HA IPs, anti-Myc IPs, and the total lysate (the input) were subjected to IB analysis with an anti-HA antibody (to detect NPC1L1-HA) and an anti-His antibody (to detect NPC2-Myc-His). Abbreviations: IB, immunoblot; IP, immunoprecipitate.

although the expression level of NPC2 mRNA was not altered by the coexpression of NPC1L1 (Fig. 2B). Because the expression of endogenous NPC1, endogenous cathepsin D (Fig. 2A), and exogenous GM2AP (Supporting Fig. 1), which are also lysosomal proteins, was hardly affected by the coexpression of NPC1L1, the reduction in the NPC2 protein level did not likely result from a nonspecific effect of NPC1L1 on lysosomal protein expression.

Maturation and Secretion of NPC2 Protein Are Inhibited by the Coexpression of NPC1L1. A detailed analysis of the molecular association between NPC1L1 and NPC2 was performed. As shown in Fig. 2C, the expression of intracellular HMW NPC2 was dramatically reduced as the expression of NPC1L1 increased. In addition, the ratio of cellular LMW NPC2 to cellular HMW NPC2 was elevated by the increase in the expression of NPC1L1. Furthermore, because it had been reported that NPC2 is secreted extracellularly,[24,25] we also analyzed the effect of NPC1L1 on NPC2 secretion. As shown in Fig. 2C, the amount of NPC2 secreted into media was decreased by NPC1L1

ID: nagarajulum | Black Lining: [ON] | Time: 03:01 | Path: N:/3b2/HEP#/Vol00000/110663/APPFile/JW-HEP#110663

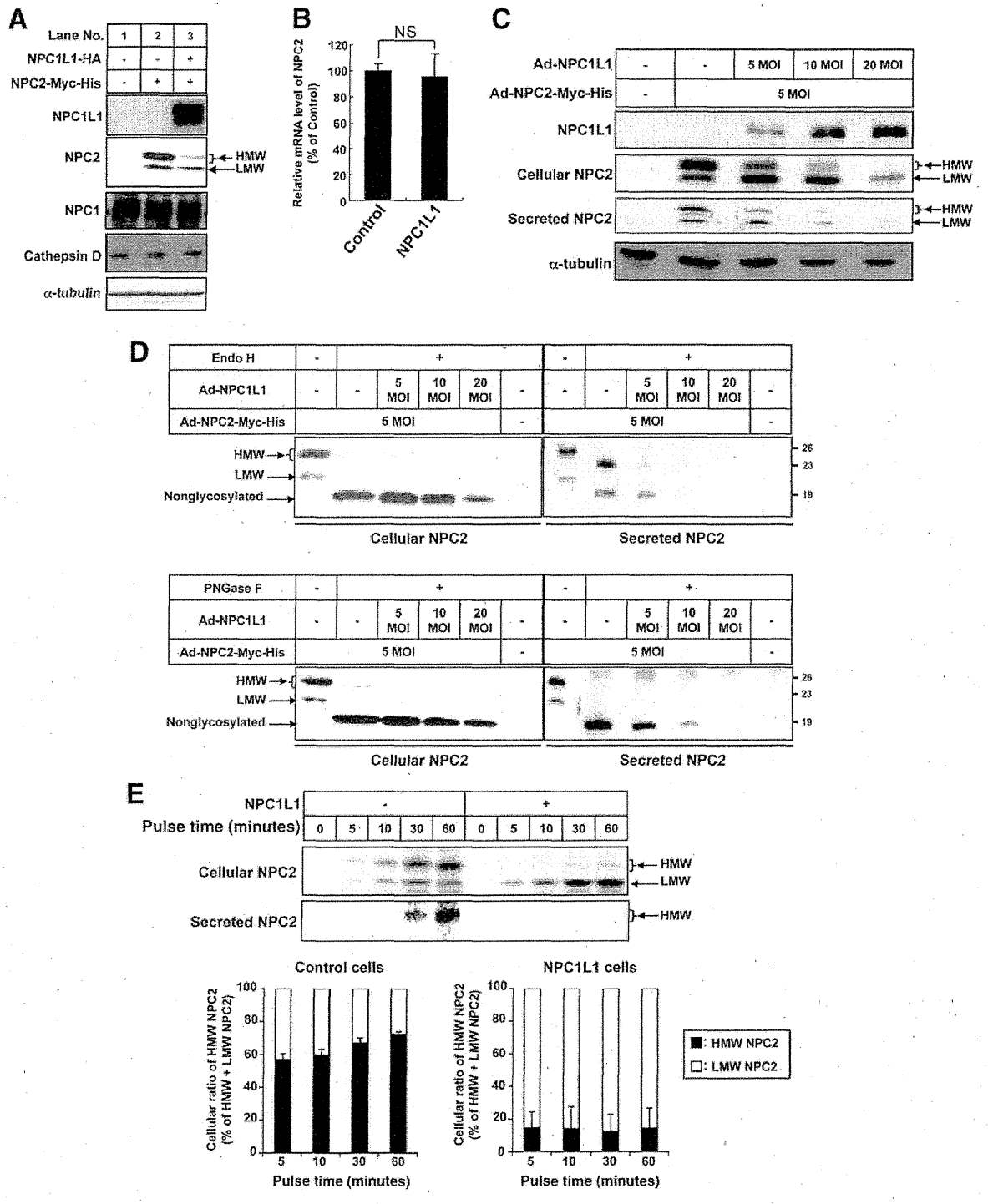

Fig. 2. Effect of NPC1L1 on the expression of NPC2. (A) CHO-K1 cells were transfected with the indicated vectors or an empty control vector. Twenty-four hours after transfection, the cells were harvested and subjected to an immunoblot analysis. (B) The mRNA levels of NPC2 in CHO-K1 cells that were cultured for 24 hours after transient transfection with the NPC2-Myc-His vector and either the NPC1L1-HA vector or an empty control vector were determined with quantitative real-time PCR. The relative mRNA level of NPC2 in each cell was normalized to the level of β-actin mRNA. The columns and vertical bars represent the means and standard deviations of three determinations. (C) CHO-K1 cells were infected with Ad-NPC1L1 at the indicated MOI together with Ad-NPC2-Myc-His at 5 MOI. Twenty-four hours after infection, the total cell lysate and the concentrated media were subjected to an immunoblot analysis. Ad-GFP was used to equalize the total amount of the infected adenovirus. (D) The aforementioned total cell lysate and concentrated media were deglycosylated with either Endo H or PNGase F (see the supporting information). The deglycosylated and undigested proteins were subjected to immunoblot analyses. (E) CHO-K1 cells were infected with Ad-NPC1L1 or Ad-GFP (the control) at 10 MOI together with Ad-NPC2-Myc-His at 5 MOI. Twenty-four hours after infection, ^{35}S-labeling was performed for the indicated times. The ^{35}S-labeled NPC2 protein was detected with a phosphor imager. The lower panels show the ratio of the ^{35}S-labeled HMW NPC2 radioactivity to the total ^{35}S-labeled NPC2 radioactivity. The data points and bars represent the means and standard deviations of three specimens on different images. Abbreviation: NS, not significant.

J_ID: ZHE Customer A_ID: 11-0942.R1 Customer Art: ZHE24772 Date: 5-November-11 Stage: Page: 5

overexpression, and this was consistent with the decrease in the intracellular NPC2 protein level.

A glycosidase digestion assay was performed next. After digestion with endoglycosidase H (Endo H; upper panels, Fig. 2D) or peptide *N*-glycosidase F (PNGase F; lower panels, Fig. 2D), intracellular NPC2 was detected at 18 kDa, which corresponded to the nonglycosylated form of the protein. This result suggests that HMW NPC2 and LMW NPC2 are glycosylation variants. In addition, the secretion of maturely glycosylated HMW NPC2, which corresponded to a 23-kDa band after digestion with Endo H, was concomitantly reduced with the increase in NPC1L1 expression (upper panels, Fig. 2D). These results raise the possibility that NPC1L1 inhibits the maturation of NPC2.

To test this hypothesis, we characterized NPC2 maturation over time with a [^{35}S]methionine/cysteine pulse-chase experiment. In control cells, the amounts of both cellular and secreted ^{35}S-labeled HMW NPC2 increased in a time-dependent manner (upper panels, Fig. 2E). However, in NPC1L1-overexpressing cells, very little cellular or secreted ^{35}S-labeled HMW NPC2 was detected, whereas the amount of ^{35}S-labeled LMW NPC2 increased in a time-dependent manner (upper panels, Fig. 2E). Furthermore, the ratio of the cellular amount of ^{35}S-labeled HMW NPC2 to the amount of total ^{35}S-labeled NPC2 (HMW + LMW) increased time-dependently in control cells, whereas this ratio did not change in NPC1L1-overexpressing cells (lower panels, Fig. 2E). These results support the hypothesis that NPC1L1 inhibits the maturation of NPC2 from LMW forms to HMW forms.

NPC1L1 Interacts With NPC2 in Prelysosomal Compartments. To clarify the cellular compartment in which the interaction between NPC1L1 and NPC2 occurs, we performed immunohistochemical staining for markers of various organelles. As shown in Fig. 3, NPC2 was localized in vesicle-like structures that were partially costained for the lysosomal marker cathepsin D (Fig. 3A) but not for the endoplasmic reticulum (ER) marker calnexin (Fig. 3B). However, in agreement with the results of the immunoblot analyses (Figs. 1 and 2A), when NPC1L1 was overexpressed, the expression of NPC2 protein was reduced, and minimal staining of NPC2 was observed (Fig. 3C).

Because treatment with *N*-(benzyloxycarbonyl)leucinylleucinylleucinal (MG132), a proteasome inhibitor, could inhibit the degradation of NPC2 and increase LMW NPC2 even when NPC1L1 was overexpressed (Supporting Fig. 2), immunohistochemical staining was performed in the presence of MG132. Figure 3D shows that MG132-sensitive NPC2 was colocalized with NPC1L1 in intracellular compartments that were partially costained for calnexin (Fig. 3E) but not cathepsin D (Fig. 3F). The observation that NPC1L1 could be coimmunoprecipitated with LMW NPC2 (Fig. 1) and the observation that most of the MG132-sensitive NPC2 was LMW NPC2 (Supporting Fig. 2) suggest that NPC1L1 interacts with LMW NPC2 in prelysosomal compartments, including the ER.

Degradation of NPC2 Is Accelerated in the Presence of NPC1L1. Because NPC1L1 reduces the expression of NPC2 protein, it was hypothesized that the degradation of NPC2 protein is accelerated by NPC1L1. To test this hypothesis, we analyzed the degradation rate of NPC2 protein. As shown in Fig. 4, the degradation of LMW NPC2 was more rapid in NPC1L1-overexpressing cells (half-life = 2.1 ± 0.1 hours) versus control cells (half-life = 7.1 ± 2.5 hours). In contrast, the half-life of HMW NPC2 was hardly affected by the overexpression of NPC1L1 (3.2 ± 0.8 hours in control cells and 2.3 ± 0.1 hours in NPC1L1-overexpressing cells). These results suggest that the ability of NPC1L1 to accelerate the degradation of LMW NPC2 may contribute to the lower expression of NPC2 protein in NPC1L1-overexpressing cells and that the reduced expression of HMW NPC2 in NPC1L1-overexpressing cells (Figs. 1 and 2A,C) could be explained by the inhibition of NPC2 maturation rather than the difference in the degradation speed of HMW NPC2.

Endogenous NPC1L1 Regulates the Protein Expression and Secretion of NPC2. Although the overexpression of NPC1L1 caused a reduction in the protein expression and secretion of NPC2, an overexpression model is fraught with potential artifacts. To eliminate this possibility, we investigated the ability of endogenous NPC1L1 to regulate the expression and secretion of endogenous NPC2. For this purpose, HepG2 cells in which both NPC1L1 and NPC2 were expressed endogenously were transfected with a small interfering RNA targeted against Niemann-Pick C1-like 1 (siNPC1L1), and changes in NPC2 expression and secretion were analyzed. As shown in Fig. 5, after the transfection of siNPC1L1, the mRNA levels of endogenous NPC1L1 (Fig. 5A) and its protein levels (Fig. 5B) were reduced to approximately 40% and 60%, respectively, of the levels in cells transfected with the control small interfering RNA (siControl). Under these conditions, although the expression of NPC2 mRNA was unaltered (Fig. 5A), the level of NPC2 protein increased more than 1.9-fold (cellular NPC2, Fig. 5B). In addition, the amount of NPC2 secreted

ID: nagarajulum | Black Lining: [ON] | Time: 03:01 | Path: N:/3b2/HEP#/Vol00000/110663/APPFile/JW-HEP#110663

J_ID: ZHE Customer A_ID: 11-0942.R1 Customer Art: ZHE24772 Date: 5-November-11 Stage: Page: 6

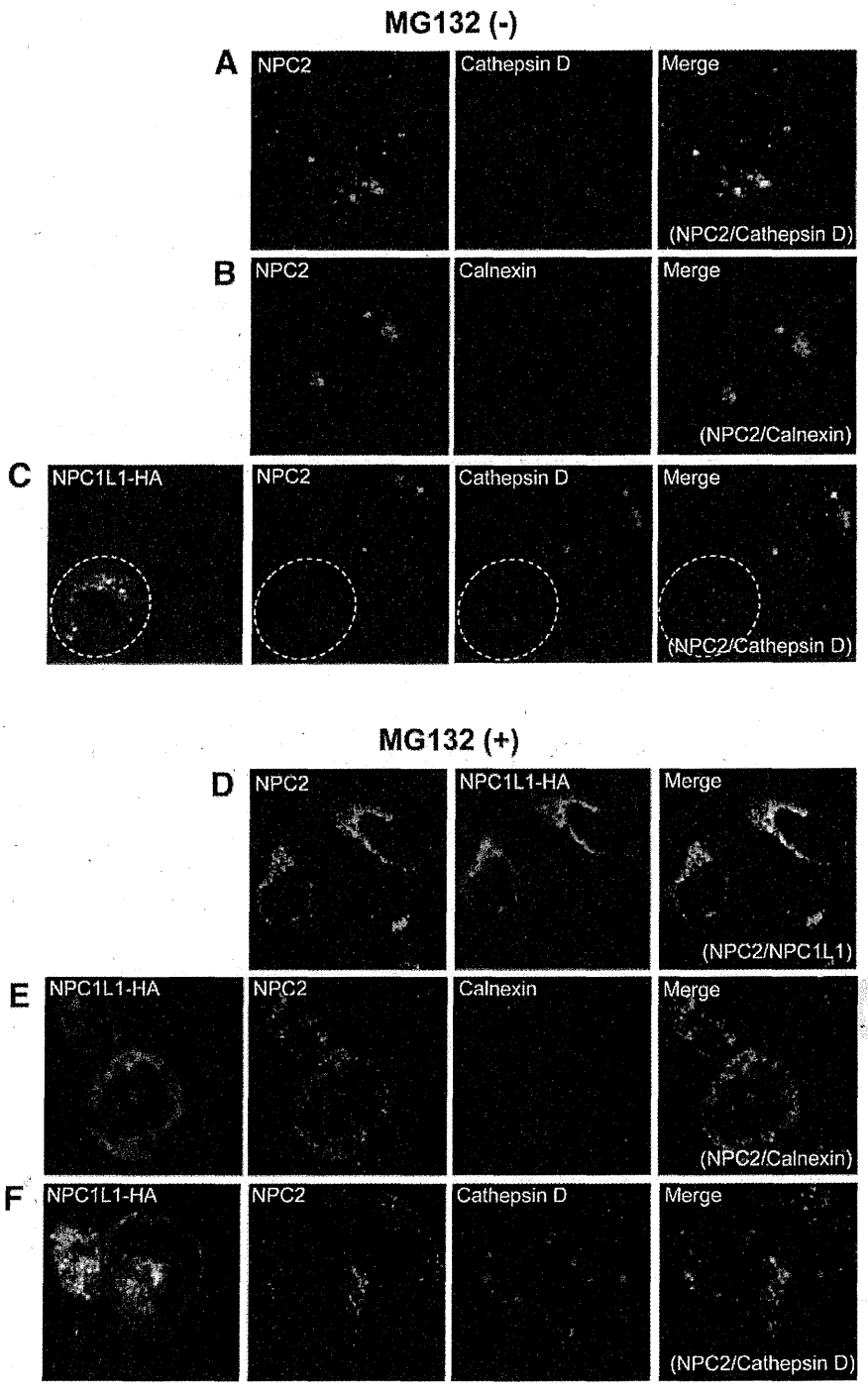

COLOR

Fig. 3. Intracellular colocalization of NPC1L1 with NPC2 in HepG2 cells. The cellular localization of NPC1L1-HA and NPC2 was examined with immunohistochemical staining. HepG2 cells were transfected with (A,B) the control vector or (C) the NPC1L1-HA vector. Twenty-four hours after transfection, the cells were stained for an immunohistochemical analysis. NPC1L1-expressing cells are indicated by circles. (D-F) HepG2 cells were transfected with the NPC1L1-HA vector. Twenty-four hours after transfection, the cells were treated with MG132 (10 μM) for 6 hours, and they were then subjected to immunohistochemical staining. Representative images are shown. In each panel, colocalization appears yellow in the merged image.

into the media also increased more than 2.5-fold after the suppression of NPC1L1 expression (secreted NPC2, Fig. 5B). However, transfection with siNPC1L1 had no effect on NPC1 protein expression (Fig. 5B). These results suggest that the expression and secretion of endogenous NPC2 are negatively regulated by endogenous NPC1L1.

Suppression of Intracellular Cholesterol Trafficking by NPC1L1 Overexpression Can Be Rescued by the Addition of Purified NPC2 Protein. Because the loss of intracellular NPC2 suppresses intracellular cholesterol trafficking and causes cholesterol accumulation within lysosomes,[10] the cholesterol distribution was analyzed in NPC1L1-overexpressing cells. In agreement

ID: nagarajulum | Black Lining: [ON] | Time: 03:01 | Path: N:/3b2/HEP#/Vol00000/110663/APPFile/JW-HEP#110663

J_ID: ZHE Customer A_ID: 11-0942.R1 Customer Art: ZHE24772 Date: 5-November-11 Stage: Page: 7

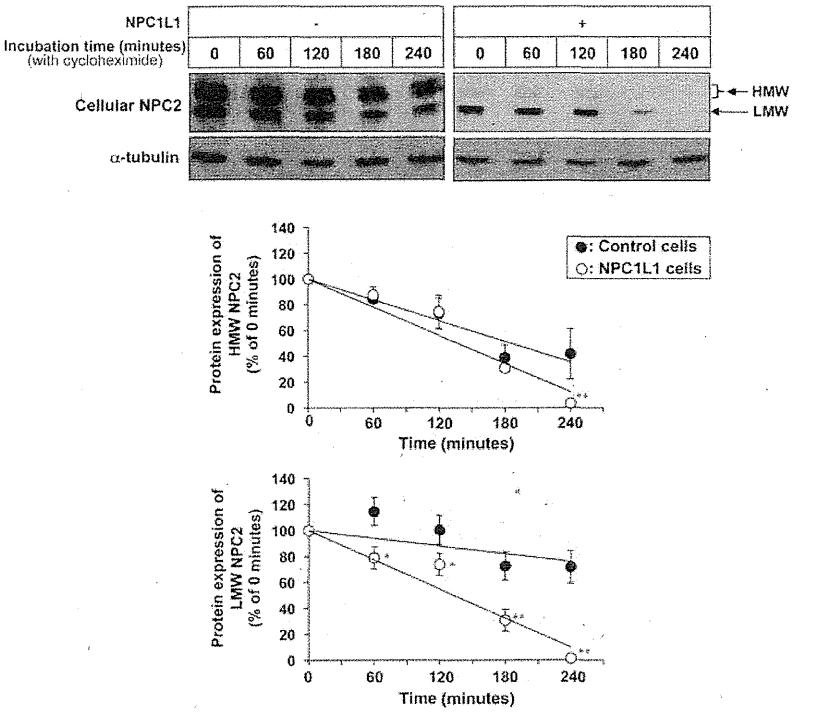

Fig. 4. Effect of NPC1L1 on the degradation rate of NPC2 protein. CHO-K1 cells were infected with Ad-NPC1L1 or Ad-GFP (the control) at 10 MOI together with Ad-NPC2-Myc-His at 5 MOI. Twenty-four hours after infection, the cells were incubated with cycloheximide (100 μM). The total cell lysate, which was prepared at the indicated time points, was examined with an immunoblot analysis. The lower panels show quantitative comparisons of the levels of NPC2 protein normalized to the level of α-tubulin. The data points and bars represent the means and standard deviations of three specimens on different immunoblots. *Significantly different from control cells according to the Student t test ($P < 0.05$). **Significantly different from control cells according to the Student t test ($P < 0.01$).

with the previous results, the amount of endogenous NPC2 protein in HepG2 cells was reduced along with the increase in NPC1L1 expression, whereas the level of endogenous NPC1 protein was hardly affected (Fig. 6A). Because extracellular (secreted) NPC2 can be taken up into lysosomes via receptor-mediated endocytosis,[26] NPC1L1-overexpressing cells were cultured in media containing exogenous NPC2 protein, and the amount of cellular NPC2 was examined. Exogenous NPC2 protein was purified from cell culture media containing secreted HMW NPC2. Figure 6B shows that the reduction of NPC2 in NPC1L1-overexpressing cells could be recovered by culturing with purified NPC2 protein, and this suggests that NPC1L1 may only minimally affect the protein stability of endocytosed NPC2. The endocytosed NPC2 protein in NPC1L1-overexpressing cells was colocalized with the lysosomal marker cathepsin D by immunohistochemistry (data not shown). These results are consistent with the observation that NPC1L1 interacts with NPC2 in prelysosomal compartments (Fig. 3E).

Filipin staining was next performed in order to analyze the cellular distribution of cholesterol. As shown in Fig. 6C, in comparison with control cells, NPC1L1-overexpressing cells exhibited increased staining for intracellular cholesterol, whereas staining for cholesterol in the plasma membrane was reduced. A similar pattern was observed in cells treated with U18666A, an inhibitor of intracellular cholesterol trafficking. When NPC1L1-overexpressing cells were incubated with purified wild-type (WT) NPC2, intracellular NPC2 levels were restored to the same levels found in control cells (Fig. 6B); intracellular cholesterol accumulation was significantly decreased, and in turn, the distribution of cholesterol in the plasma membrane was restored (Fig. 6C). This rescue effect was not observed when cells were cultured with NPC2 D72A, a loss-of-function mutant.[27] These results suggest that the altered distribution of cholesterol in NPC1L1-overexpressing cells is mostly caused by the reduced expression of lysosomal NPC2 and not by NPC1L1 itself. In addition, NPC1L1 only slightly affects the function of lysosomal NPC2.

NPC2 Expression Is Negatively Correlated With NPC1L1 in Human Liver Specimens. Finally, the correlation between the levels of NPC2 and NPC1L1 in human liver specimens was determined with immunoblot analyses and quantitative real-time PCR. In agreement with the *in vitro* results, the protein levels of NPC2 were negatively correlated with NPC1L1 levels in human liver specimens (Fig. 7A), although there was no significant correlation between the mRNA levels (Fig. 7B). Furthermore, the translational efficiency of NPC2, which is expressed as the ratio of the NPC2 protein level to the NPC2 mRNA level, was also negatively correlated with the protein level of NPC1L1

ID: nagarajulum | Black Lining: [ON] | Time: 03:01 | Path: N:/3b2/HEP#/Vol00000/110663/APPFile/JW-HEP#110663

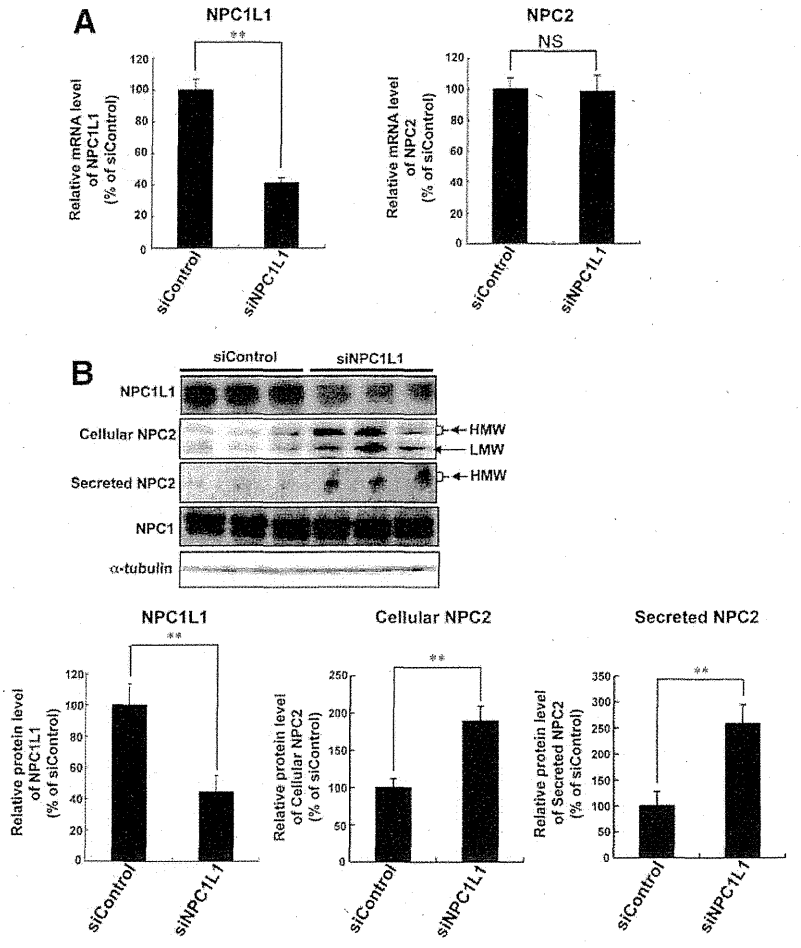

Fig. 5. Effect of siNPC1L1 on the endogenous expression of NPC2. HepG2 cells were transfected with siNPC1L1 or siControl (see the supporting information) and cultured for 2 days. The extracted RNA and the total cell lysate were then analyzed with (A) quantitative real-time PCR and (B) an immunoblot analysis, respectively. (A) The relative mRNA levels of NPC1L1 and NPC2 were normalized to the β-actin mRNA levels. (B) The relative levels of the NPC1L1 and NPC2 proteins were calculated as the band densities of the proteins and were normalized to the α-tubulin protein level in each specimen. The columns and vertical bars represent the means and standard deviations of the three specimens in the immunoblot. **Significantly different according to the Student t test ($P < 0.01$). Abbreviation: NS, not significant.

(Fig. 7C). These results support the hypothesis that the protein expression of NPC2 is posttranscriptionally regulated by NPC1L1 in the human liver.

Discussion

According to this study, in addition to its well-known role as a cholesterol importer, NPC1L1 has a novel function as a negative regulator of the expression and secretion of NPC2, which is based on the ability of NPC1L1 to inhibit the maturation of NPC2 protein and stimulate the degradation of LMW NPC2 protein. Because treatment with ezetimibe, an inhibitor of NPC1L1-mediated cholesterol import, does not affect the binding of NPC1L1 and NPC2 and cannot reverse the reduction in the NPC2 protein level in NPC1L1-coexpressing cells (Supporting Fig. 3), this novel function of NPC1L1 as a negative regulator of NPC2 protein is independent of its well-known role as a cholesterol importer.

Previously, it has been reported that NPC2 is degraded by the proteasome system.[22] Therefore, we investigated whether treatment with MG132, a proteasome inhibitor, could inhibit the NPC1L1-mediated down-regulation of NPC2. In agreement with the previous report,[22] in the absence of NPC1L1, the levels of both HMW NPC2 and LMW NPC2 were increased by MG132 treatment (Supporting Fig. 2). However, when NPC1L1 was coexpressed, MG132 treatment hardly increased the expression of HMW NPC2, although the expression of LMW NPC2 clearly increased (Supporting Fig. 2). This observation is in agreement with the finding that NPC1L1 inhibits the maturation of NPC2 from LMW forms to HMW forms (Fig. 2C,E). Furthermore, the stability of LMW NPC2 was altered by NPC1L1 coexpression (Fig. 4), and LMW NPC2 coimmunoprecipitated with NPC1L1 (Fig. 1). These data imply that NPC1L1 interacts with LMW NPC2, inhibits its maturation, and simultaneously promotes its degradation. As a

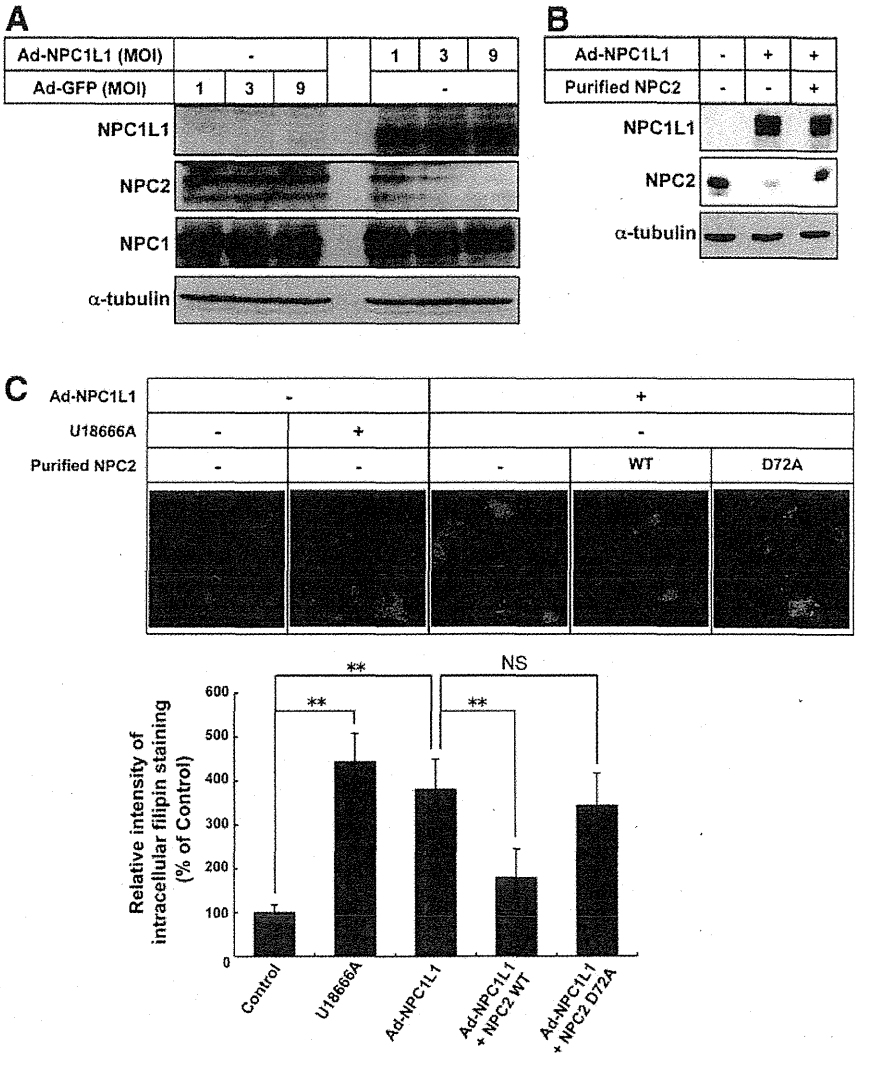

Fig. 6. Effect of NPC1L1 on intracellular cholesterol trafficking. (A) HepG2 cells were infected with Ad-NPC1L1 or Ad-GFP at the indicated MOI. Twenty-four hours after infection, the cells were collected and subjected to an immunoblot analysis. (B) HepG2 cells were infected with Ad-NPC1L1 or Ad-GFP (the control) at 3 MOI and were cultured together with purified NPC2 protein (10 nM). Twenty-four hours after infection, the cells were collected and subjected to an immunoblot analysis. (C) HepG2 cells were infected with Ad-NPC1L1 or Ad-GFP (the control) at 3 MOI and were cultured together with the indicated type of purified NPC2 protein (10 nM) for 24 hours or with U18666A (1.25 μM) for 8 hours. Twenty-four hours after infection, the cells were stained with filipin. The upper panels show the results of filipin staining. Representative images are shown. The lower panel shows a quantitative comparison of filipin staining in intracellular compartments. The columns and vertical bars represent means and standard deviations of three different images. **Significantly different according to an analysis of variance followed by Dunnett's test ($P < 0.01$). Abbreviation: NS, not significant.

result, intracellular NPC2 is reduced, and this in turn leads to a decrease in NPC2 secretion (Fig. 8).

In contrast to LMW NPC2, a molecular association between HMW NPC2 and NPC1L1 was not detected by coimmunoprecipitation (Fig. 1). Because HMW NPC2 and LMW NPC2 are glycosylation variants (Fig. 2D), it is possible that the complex glycosylation of HMW NPC2 may inhibit its binding to NPC1L1, whereas core-glycosylated NPC2 can interact with NPC1L1. This idea is consistent with the observation that in addition to the expression of WT NPC2, the expression of NPC2 mutants (in which one or both of the glycosylation sites of NPC2 are mutated[24]) was reduced by the coexpression of NPC1L1 (Supporting Fig. 4). Because NPC1L1 colocalizes with NPC2 in prelysosomal compartments (Fig. 3) and the reduced expression of NPC2 can be rescued by exogenous secreted NPC2 (Fig. 6B), it seems that NPC1L1 interacts with NPC2 during the process of complex glycosylation.

The RNA interference studies using HepG2 cells (Fig. 5) and the correlation analysis of the expression levels of NPC1L1 and NPC2 in human liver specimens (Fig. 7) have revealed that endogenous NPC1L1 negatively regulates the expression of NPC2 posttranscriptionally. It has recently been reported that in addition to the NPC1L1-mediated regulation of NPC2, Nogo-B receptor (NgBR) interacts with NPC2 at the ER and enhances NPC2 protein stability by inhibiting its proteasomal degradation.[22] Because NgBR is known to be expressed in the liver,[28] NgBR may function as a positive regulator of NPC2 protein expression, whereas NPC1L1 acts as a negative regulator. The balance of the expression levels of NPC1L1 and

J_ID: ZHE Customer A_ID: 11-0942.R1 Customer Art: ZHE24772 Date: 5-November-11 Stage: Page: 10

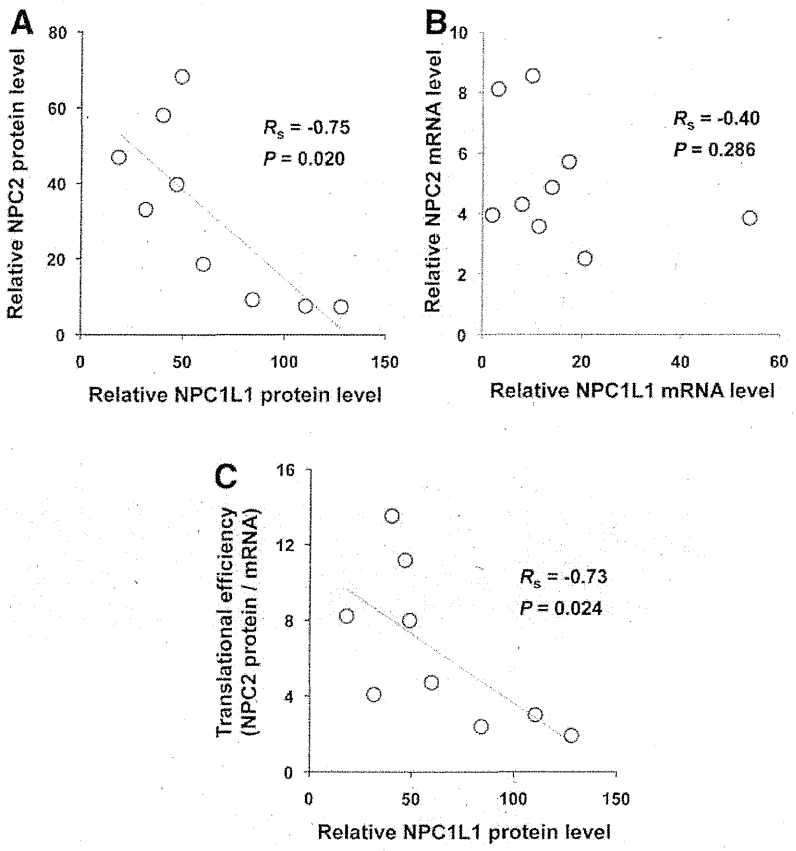

Fig. 7. Correlation between the levels of NPC1L1 and NPC2 in human liver specimens. Homogenates and extracted RNA from human liver specimens were subjected to (A) an immunoblot analysis and (B) quantitative real-time PCR, respectively. (A) The relative protein levels of NPC1L1 and NPC2 were calculated as the band densities of the proteins and were normalized to the α-tubulin protein level in each specimen. (B) The relative mRNA levels of NPC1L1 and NPC2 were normalized to the β-actin mRNA level in each specimen. (C) The translational efficiency of NPC2 was calculated as the ratio of the NPC2 protein level to the NPC2 mRNA level. A correlation analysis was performed with Spearman's rank method. Abbreviation: R_s, Spearman's rank correlation coefficient.

NgBR may, therefore, determine the hepatic expression of NPC2 protein.

In addition to posttranscriptional modification, several groups have studied the transcriptional regulation of the NPC2 gene. For instance, Rigamonti et al.[29] reported that in human macrophages, NPC2 mRNA is induced by activators of liver X receptor (LXR). Because LXR is activated by cellular cholesterol-related compounds, the expression of NPC2 mRNA may be positively regulated by cellular cholesterol levels. On the other hand, cholesterol has been shown to down-regulate the expression of NPC1L1 by transcriptional regulation via sterol regulatory element binding protein 2 and hepatocyte nuclear factor 4α.[30,31] Taken together, these data suggest that when the cellular cholesterol level increases, the expression of NPC2 protein is effectively elevated by a combination of positive transcriptional regulation via the LXR pathway and reduced posttranscriptional regulation via the interaction with NPC1L1. Because NPC2 is a crucial protein for intracellular cholesterol trafficking, which affects the regulation of cholesterol synthesis and uptake by delivering cholesterol to the sterol-sensing machinery in the ER,[32] the expression level of NPC2 protein must be tightly regulated by various steps.

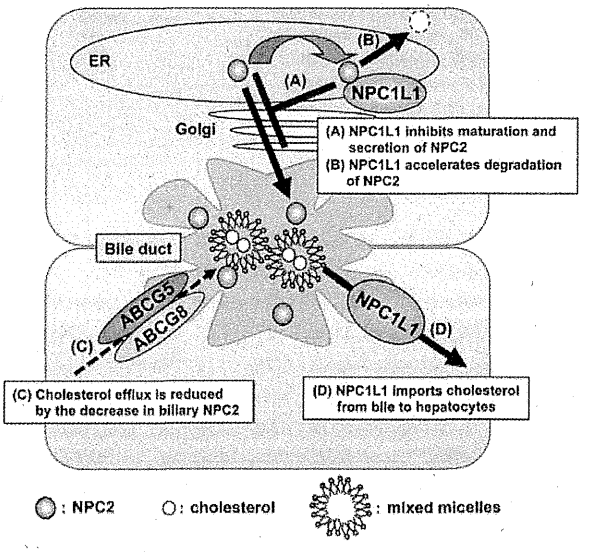

Fig. 8. Suggested function of hepatic NPC1L1 in the regulation of biliary cholesterol secretion. (A) NPC1L1 inhibits the maturation and secretion of NPC2. (B) NPC1L1 accelerates the degradation of NPC2. (C) By reducing NPC2 secretion, NPC1L1 indirectly suppresses ABCG5/ABCG8-mediated cholesterol efflux. (D) In addition to its well-known function as a cholesterol importer, NPC1L1 contributes to the regulation of biliary cholesterol secretion by negatively regulating NPC2 secretion.

COLOR

ID: nagarajulum | Black Lining: [ON] | Time: 03:02 | Path: N:/3b2/HEP#/Vol00000/110663/APPFile/JW-HEP#110663

NPC1L1 affects the secretion of NPC2 protein by inhibiting the maturation and expression of intracellular NPC2 (Figs. 2C and 5). This regulatory mechanism of NPC2 secretion would be relevant in specific tissues such as the liver and intestine because NPC1L1 is predominantly expressed in these tissues in humans. In fact, because of the negative correlation between the protein levels of NPC1L1 and NPC2 in human liver specimens (Fig. 7), it is possible that hepatic NPC1L1 negatively regulates the biliary secretion of NPC2. Our recent study revealed the physiological function of biliary NPC2 as a positive regulator of biliary cholesterol secretion mediated by ABCG5/ABCG8 on the bile canalicular membrane of hepatocytes.[15] Together with the results from this study, the data suggest that hepatic NPC1L1 may also indirectly affect ABCG5/ABCG8-mediated transport by decreasing biliary NPC2. In addition to its direct role in cholesterol re-uptake from the bile by hepatocytes,[6] NPC1L1 may down-regulate the biliary secretion of NPC2 and, consequently, reduce NPC2-mediated cholesterol efflux by ABCG5/ABCG8 from hepatocytes into the bile[15] (Fig. 8). When we consider that ABCG5 and ABCG8 are predominantly expressed in the liver and intestine and that ABCG5/ABCG8-mediated cholesterol excretion is an important process in cholesterol homeostasis, it makes sense that the regulatory mechanism for the secretion of NPC2 is working in these tissues to maintain adequate cholesterol levels in response to the dynamic cholesterol fluctuations in the body.

Collectively, the results of the present study suggest that NPC1L1 down-regulates the expression and secretion of NPC2 by interacting with NPC2 during its maturation process. Through this regulatory function, hepatic NPC1L1 is suggested to suppress the hepatic expression and biliary secretion of NPC2. In addition to its direct role in cholesterol re-uptake, hepatic NPC1L1 may effectively control biliary cholesterol secretion by negatively regulating NPC2 secretion because biliary NPC2 stimulates ABCG5/ABCG8-mediated cholesterol efflux.[15] This is the first report suggesting a function for NPC1L1 besides its activity as a (re-)uptake transporter.

References

1. Altmann SW, Davis HR Jr, Zhu LJ, Yao X, Hoos LM, Tetzloff G, et al. Niemann-Pick C1 like 1 protein is critical for intestinal cholesterol absorption. Science 2004;303:1201-1204.
2. Yamanashi Y, Takada T, Suzuki H. Niemann-Pick C1-like 1 overexpression facilitates ezetimibe-sensitive cholesterol and beta-sitosterol uptake in CaCo-2 cells. J Pharmacol Exp Ther 2007;320:559-564.
3. Davies JP, Scott C, Oishi K, Liapis A, Ioannou YA. Inactivation of NPC1L1 causes multiple lipid transport defects and protects against diet-induced hypercholesterolemia. J Biol Chem 2005;280: 12710-12720.
4. Sane AT, Sinnett D, Delvin E, Bendayan M, Marcil V, Menard D, et al. Localization and role of NPC1L1 in cholesterol absorption in human intestine. J Lipid Res 2006;47:2112-2120.
5. Matsuo H, Takada T, Ichida K, Nakamura T, Nakayama A, Ikebuchi Y, et al. Common defects of ABCG2, a high-capacity urate exporter, cause gout: a function-based genetic analysis in a Japanese population. Sci Transl Med 2009;1:5ra11.
6. Temel RE, Tang W, Ma Y, Rudel LL, Willingham MC, Ioannou YA, et al. Hepatic Niemann-Pick C1-like 1 regulates biliary cholesterol concentration and is a target of ezetimibe. J Clin Invest 2007;117: 1968-1978.
7. Davies JP, Levy B, Ioannou YA. Evidence for a Niemann-Pick C (NPC) gene family: identification and characterization of NPC1L1. Genomics 2000;65:137-145.
8. Vanier MT, Millat G. Niemann-Pick disease type C. Clin Genet 2003; 64:269-281.
9. Carstea ED, Morris JA, Coleman KG, Loftus SK, Zhang D, Cummings C, et al. Niemann-Pick C1 disease gene: homology to mediators of cholesterol homeostasis. Science 1997;277:228-231.
10. Naureckiene S, Sleat DE, Lackland H, Fensom A, Vanier MT, Wattiaux R, et al. Identification of HE1 as the second gene of Niemann-Pick C disease. Science 2000;290:2298-2301.
11. Vanier MT, Millat G. Structure and function of the NPC2 protein. Biochim Biophys Acta 2004;1685:14-21.
12. Infante RE, Wang ML, Radhakrishnan A, Kwon HJ, Brown MS, Goldstein JL. NPC2 facilitates bidirectional transfer of cholesterol between NPC1 and lipid bilayers, a step in cholesterol egress from lysosomes. Proc Natl Acad Sci U S A 2008;105:15287-15292.
13. Wang ML, Motamed M, Infante RE, Abi-Mosleh L, Kwon HJ, Brown MS, et al. Identification of surface residues on Niemann-Pick C2 essential for hydrophobic handoff of cholesterol to NPC1 in lysosomes. Cell Metab 2010;12:166-173.
14. Klein A, Amigo L, Retamal MJ, Morales MG, Miquel JF, Rigotti A, et al. NPC2 is expressed in human and murine liver and secreted into bile: potential implications for body cholesterol homeostasis. HEPATOLOGY 2006;43:126-133.
15. Yamanashi Y, Takada T, Yoshikado T, Shoda J, Suzuki H. NPC2 regulates biliary cholesterol secretion via stimulation of ABCG5/G8-mediated cholesterol transport. Gastroenterology 2011;140:1664-1674.
16. Yu L, Hammer RE, Li-Hawkins J, Von Bergmann K, Lutjohann D, Cohen JC, et al. Disruption of Abcg5 and Abcg8 in mice reveals their crucial role in biliary cholesterol secretion. Proc Natl Acad Sci U S A 2002;99:16237-16242.
17. Vuoristo M, Miettinen TA. Absorption, metabolism, and serum concentrations of cholesterol in vegetarians: effects of cholesterol feeding. Am J Clin Nutr 1994;59:1325-1331.
18. Dixit SS, Sleat DE, Stock AM, Lobel P. Do mammalian NPC1 and NPC2 play a role in intestinal cholesterol absorption? Biochem J 2007; 408:1-5.
19. Narushima K, Takada T, Yamanashi Y, Suzuki H. Niemann-Pick C1-like 1 mediates alpha-tocopherol transport. Mol Pharmacol 2008;74: 42-49.
20. Yamanashi Y, Takada T, Suzuki H. In-vitro characterization of the six clustered variants of NPC1L1 observed in cholesterol low absorbers. Pharmacogenet Genomics 2009;19:884-892.
21. Ikebuchi Y, Takada T, Ito K, Yoshikado T, Anzai N, Kanai Y, et al. Receptor for activated C-kinase 1 regulates the cellular localization and function of ABCB4. Hepatol Res 2009;39:1091-1107.
22. Harrison KD, Miao RQ, Fernandez-Hernando C, Suarez Y, Davalos A, Sessa WC. Nogo-B receptor stabilizes Niemann-Pick type C2 protein and regulates intracellular cholesterol trafficking. Cell Metab 2009;10: 208-218.

23. Pipalia NH, Huang A, Ralph H, Rujoi M, Maxfield FR. Automated microscopy screening for compounds that partially revert cholesterol accumulation in Niemann-Pick C cells. J Lipid Res 2006;47:284-301.
24. Chikh K, Vey S, Simonot C, Vanier MT, Millat G. Niemann-Pick type C disease: importance of N-glycosylation sites for function and cellular location of the NPC2 protein. Mol Genet Metab 2004;83:220-230.
25. Mutka AL, Lusa S, Linder MD, Jokitalo E, Kopra O, Jauhiainen M, et al. Secretion of sterols and the NPC2 protein from primary astrocytes. J Biol Chem 2004;279:48654-48662.
26. Willenborg M, Schmidt CK, Braun P, Landgrebe J, von Figura K, Saftig P, et al. Mannose 6-phosphate receptors, Niemann-Pick C2 protein, and lysosomal cholesterol accumulation. J Lipid Res 2005;46:2559-2569.
27. Ko DC, Binkley J, Sidow A, Scott MP. The integrity of a cholesterol-binding pocket in Niemann-Pick C2 protein is necessary to control lysosome cholesterol levels. Proc Natl Acad Sci U S A 2003;100: 2518-2525.
28. Miao RQ, Gao Y, Harrison KD, Prendergast J, Acevedo LM, Yu J, et al. Identification of a receptor necessary for Nogo-B stimulated chemotaxis and morphogenesis of endothelial cells. Proc Natl Acad Sci U S A 2006;103:10997-11002.
29. Rigamonti E, Helin L, Lestavel S, Mutka AL, Lepore M, Fontaine C, et al. Liver X receptor activation controls intracellular cholesterol trafficking and esterification in human macrophages. Circ Res 2005;97: 682-689.
30. Alrefai WA, Annaba F, Sarwar Z, Dwivedi A, Saksena S, Singla A, et al. Modulation of human Niemann-Pick C1-like 1 gene expression by sterol: role of sterol regulatory element binding protein 2. Am J Physiol Gastrointest Liver Physiol 2007;292:G369-G376.
31. Iwayanagi Y, Takada T, Suzuki H. HNF4α is a crucial modulator of the cholesterol-dependent regulation of NPC1L1. Pharm Res 2008;25: 1134-1141.
32. Frolov A, Zielinski SE, Crowley JR, Dudley-Rucker N, Schaffer JE, Ory DS. NPC1 and NPC2 regulate cellular cholesterol homeostasis through generation of low density lipoprotein cholesterol-derived oxysterols. J Biol Chem 2003;278:25517-25525.

J Gastroenterol
DOI 10.1007/s00535-012-0552-9

ORIGINAL ARTICLE—LIVER, PANCREAS, AND BILIARY TRACT

Nrf2 inhibits hepatic iron accumulation and counteracts oxidative stress-induced liver injury in nutritional steatohepatitis

Kosuke Okada · Eiji Warabi · Hirokazu Sugimoto · Masaki Horie · Katsutoshi Tokushige · Tetsuya Ueda · Nobuhiko Harada · Keiko Taguchi · Etsuko Hashimoto · Ken Itoh · Tetsuro Ishii · Hirotoshi Utsunomiya · Masayuki Yamamoto · Junichi Shoda

Received: 21 November 2011 / Accepted: 25 January 2012

Abstract

Background The transcription factor nuclear factor-E2-related factor-2 (Nrf2) is a key regulator for induction of hepatic antioxidative stress systems. We aimed to investigate whether activation of Nrf2 protects against steatohepatitis.

Method Wild-type mice (WT), *Nrf2* gene-null mice (*Nrf2*-null) and *Keap1* gene-knockdown mice (*Keap1*-kd), which represent the sustained activation of Nrf2, were fed a methionine- and choline-deficient diet (MCDD) for 13 weeks and analyzed.

Results In *Keap1*-kd fed an MCDD, steatohepatitis did not develop over the observation periods; however, in *Nrf2*-null fed an MCDD, the pathological state of the steatohepatitis was aggravated in terms of fatty change, inflammation, fibrosis and iron accumulation. In WT mice fed an MCDD, Nrf2 and antioxidative stress genes regulated by Nrf2 were potently activated in the livers, and in *Keap1*-kd, their basal levels were potently activated. Oxidative stress was significantly increased in the livers of the *Nrf2*-null and suppressed in the livers of the *Keap1*-kd compared to that of WT, based on the levels of 4-hydroxy-2-nonenal and malondialdehyde. Iron accumulation was greater in the livers of the *Nrf2*-null mice compared to those of the WT mice, and it was not observed in *Keap1*-kd. Further, the iron release from the isolated hepatocyte of *Nrf2*-null mice was significantly decreased. Sulforaphane, an activator of Nrf2, suppressed the pathological states and oxidative stress in the livers.

Conclusions Nrf2 has protective roles against nutritional steatohepatitis through inhibition of hepatic iron accumulation and counteraction against oxidative stress-induced liver injury. Nrf2 activation by pharmaceutical intervention could be a new option for the prevention and treatment of steatohepatitis.

Keywords *Nrf2* gene-knockout mouse · *Keap1* gene-knockdown mouse · Methionine- and choline-deficient diet · Iron metabolism

K. Okada · M. Horie · J. Shoda (✉)
Field of Basic Sports Medicine, Sports Medicine,
Faculty of Medicine, Graduate School of Comprehensive
Human Sciences, The University of Tsukuba, Tsukuba,
Ibaraki 305-8574, Japan
e-mail: shodaj@md.tsukuba.ac.jp

E. Warabi · T. Ishii
Biomedical Sciences, Faculty of Medicine, The University
of Tsukuba, Tsukuba, Ibaraki 305-8575, Japan

H. Sugimoto
Department of Gastroenterology, Faculty of Medicine,
The University of Tsukuba, Tsukuba, Ibaraki 305-8575, Japan

K. Tokushige · E. Hashimoto
Department of Internal Medicine and Gastroenterology,
Tokyo Women's Medical University, Shinjuku-ku,
Tokyo 162-8666, Japan

T. Ueda
Drug Development Service Division, Pharmacodynamics Group,
Medi-Chem Business Segment, Mitsubishi Chemical Medience
Corporation, Itabashi-ku, Tokyo 174-8555, Japan

N. Harada · K. Itoh
Department of Stress Response Science, Hirosaki University
Graduate School of Medicine, Zaifu-cho, Hiroksaki, Aomori
036-8562, Japan

K. Taguchi · M. Yamamoto
Department of Medical Biochemistry, Tohoku University
Graduate School of Medicine, Sendai, Miyagi 980-8675, Japan

H. Utsunomiya
Department of Strategic Surveillance for Functional Food and
Comprehensive Traditional Medicine, Wakayama Medical
University, Wakayama 641-0012, Japan

Journal : Large 535 | Dispatch : 9-2-2012 | Pages : 12
Article No. : 552 | ☐ LE | ☐ TYPESET
MS Code : JG-2011-11-OA-901 | ☑ CP | ☑ DISK

Abbreviations

α-Sma	Alpha-smooth muscle actin
ALP	Alkaline phosphatase
ALT	Alanine aminotransferase
AST	Aspartate aminotransferase
Fpn1	Ferroportin-1
γ-Gcs	γ-Glutamylcysteine synthetase
GSH	Glutathione
Gst	Glutathione *S*-transferase
Hamp	Hepcidin gene
4-HNE	4-Hydroxy-2-nonenal
Keap1	Kelch-like Ech-associated protein 1
MCDD	Methionine- and choline-deficient diet
MDA	Malondialdehyde
NASH	Non-alcoholic steatohepatitis
Nrf2	Nuclear factor-E2-related factor-2
Nqo1	NAD(P)H: quinone oxidoreductase 1
ROS	Reactive oxygen species
SFN	Sulforaphane
TfR	Transferrin receptor
Tgf	Transforming growth factor
WT	Wild type

Introduction

Non-alcoholic steatohepatitis (NASH), as a component of metabolic syndrome, will represent an increasingly important global public health problem [1, 2]. In epidemiology, a follow-up study of NASH patients for 10 years has shown that the disease progresses to cirrhosis in ca. 20% of the patients and leads to death caused by liver cirrhosis in 8% [3]. Therefore, treatment strategies for NASH patients are urgently needed. The increased levels of free fatty acids, non-heme iron and inflammatory cytokines in the livers provide a perpetuating and propagating mechanism for oxidative stress via the process of reactive oxygen species (ROS) production [1, 2] and thereby lipid peroxidation [4]. The role of oxidative stress in the pathogenesis of NASH has been confirmed in the experimental models of NASH, as well as in human NASH [2, 5–8]. Under the pathological conditions of accumulation of oxidative stress, hepatic stellate cells (HSCs), the major sources of collagen and other extracellular matrix proteins, are activated and then transformed into proliferative fibrogenic cells [7, 9, 10]. Thus, NASH is developed, leading to liver cirrhosis.

The transcription factor termed nuclear factor-E2-related factor-2 (Nrf2) serves as a cellular sensor for oxidative stress. Nrf2 is sequestered in the cytosol by Kelch-like Ech-associated protein (Keap1). Upon an oxidative challenge, modification of Keap1 sulfhydryl groups results in the stabilization and nuclear translocation of Nrf2 [11]. Nrf2 plays crucial roles for antioxidant responsive element/electrophile-responsive element (ARE/EpRE)-mediated induction of antioxidative stress genes [12]. Our previous studies have shown that chemicals and drugs activating the Nrf2 regulatory pathway are shown to decrease oxidative stress, which in turn is implicated in the pathogenesis of numerous liver diseases [13, 14]. Moreover, our and other laboratories have shown that deletion of Nrf2 leads to severe progression of nutritional steatohepatitis [15–17]. However, the protective role of Nrf2 and the feasibility of drug therapy using Nrf2 activators against liver injuries in steatohepatitis have not yet been well elucidated.

Recently, Nrf2 has been reported to regulate iron efflux from macrophages through ferroportin-1 (Fpn1) gene transcription and control iron metabolism during inflammation [18]. Fpn1 is an iron exporter on the surface of absorptive intestinal enterocytes, macrophages, hepatocytes and placental cells, all of which release iron into plasma [19]. Iron excess in hepatocytes leads to generation of oxidative stress, cell toxicity and genotoxicity. Hepatic iron overload has been found in patients of NAFLD [5, 6], and moreover, is causatively associated with hepatic fibrosis in NASH patients [20].

In this study, we studied the protective roles of Nrf2 against the development of nutritional steatohepatitis, with special reference to iron metabolism in the livers. Wild-type mice (WT), *Nrf2* gene-null mice (*Nrf2*-null) and *Keap1* gene-knockdown mice (*Keap1*-kd), which represent the sustained activation of Nrf2, were fed a methionine- and choline-deficient diet (MCDD), which is widely used for research on steatohepatitis [7, 8]. We also studied the effect of sulforaphane (SFN), a compound in broccoli sprouts that is known to be a potent Nrf2 activator [21], on the development of steatohepatitis. We first demonstrated that Nrf2 inhibits hepatic iron accumulation and counteracts against oxidative stress-induced liver injury in steatohepatitis patients. Moreover, the treatment with SFN reduced the iron accumulation and oxidative stress in the livers by an upregulation of Nrf2, which in turn led to the decreased fibrosis. Nrf2 activation by pharmaceutical intervention could be a new option for the prevention and treatment of steatohepatitis.

Materials and methods

Animals

Male 10–12-week-old WT, *Nrf2*-null and *Keap1*-kd mice [13–15] on a C57BL/6 background were fed an MCDD or control diet (Oriental Yeast, Tokyo, Japan) for 13 weeks. At the end of the experiment, serum and liver tissue specimens were collected for analysis. SFN was mixed at 0.05% (wt/wt) in MCDD (MPBio, CA, USA) and administered. All experiments were performed under protocols

Journal : Large 535 | Dispatch : 9-2-2012 | Pages : 12
Article No. : 552 | LE | TYPESET
MS Code : JG-2011-11-OA-901 | CP | DISK

approved by the Institutional Animal Care and Use Committees of the University of Tsukuba.

Biochemical and histological analysis

Serum concentrations of aspartate aminotransferase (AST), alanine aminotransferase (ALT) and alkaline phosphatase (ALP), were measured by SRL Inc. (Tokyo, Japan). The serum concentration of hepcidin 1 was measured in the laboratories of MCProt Biotechnology (Kanazawa, Japan). Liver tissues were fixed in 10% paraformaldehyde, embedded in paraffin and stained with hematoxylin–eosin (HE), a Masson trichrome, Sirius red and Berlin blue solution.

Triglyceride concentrations, GSH levels and MDA concentrations of liver tissues

Triglyceride concentrations, glutathione (GSH) levels and malondialdehyde (MDA) concentrations of liver tissues specimens were measured as previously described [15].

Immunoblot analysis

Immunoblot analysis was performed by using liver total homogenates and nuclear fraction as previously described [13, 15, 18].

Immunohistochemistry

For immunostainings of 4-hydroxy-2-nonenal (4-HNE), 2-μm-thick tissue sections were stained using the indirect immunoperoxidase method with anti-4HNE mAb (JaiCA, Shizuoka, Japan) as previously described [15].

Real-time quantitative polymerase chain reaction

Steady-state mRNA levels in the specimens were determined by real-time quantitative PCR using recently detailed methodology [13]. Primers and probes used for this study have been described previously [13, 15, 18]. Data were normalized to the amounts of *GAPDH* present in each specimen and then averaged.

Non-heme iron contents in cells and liver tissues

Non-heme iron contents of cells and liver tissue specimens were measured as previously described [22].

Isolation and culture of primary mouse hepatocytes

Primary hepatocytes were isolated from 10- to 15-week-old C57BL6 male mice by collagenase perfusion according to the method described previously [21] with slight modification. Briefly, the liver parenchymal hepatocytes were seeded at a density of 1×10^5 cells/cm^2 with D-MEM medium supplemented with 10% FBS. From the 5th day cells were then exposed for 24 h either to control medium (D-MEM) or identical medium that was manufactured to be completely deficient in methionine and choline (MCD medium) purchased from Invitrogen. All experiments were performed at least three times using different cell culture preparations from other animals.

Iron release experiment

Iron release was measured using ^{59}FeCl as previously described [18]. The percent of iron release was calculated according to the following equation: percent ^{59}Fe release = [(cpm in medium)/(cpm in medium + cpm in cells)] × 100.

Statistics

Values are given as mean ± standard error of the mean (SEM). When two groups were compared, unpaired *t* test was used for data analysis. Multiple group comparisons were performed by two-way ANOVA. A *P* value of <0.05 was defined as statistically significant.

Results

Suppression of MCDD-induced steatohepatitis progression by Nrf2

Treating mice with MCDD for 13 weeks resulted in signs of steatohepatitis in the WT mouse livers, namely fat droplet deposition, inflammatory cell infiltration and fibrosis (Fig. 1a). These changes were more apparent in the *Nrf2*-null mouse livers than in the WT mouse livers, while the *Keap1*-kd mouse livers did not show many pathological changes in fat deposition, inflammation or fibrosis. Among other effects, the fibrosis noted in the *Nrf2*-null mouse livers was bridging fibrosis. Berlin blue staining of the liver tissue showed that iron deposition was particularly evident near blood vessels. This change reflected the intensity of inflammation and fibrosis, and was more evident in *Nrf2*-null mouse livers than in WT mouse livers. However, the change was not evident in the *Keap1*-kd mouse livers. Immunostaining with 4-HNE was performed to determine the presence of lipid peroxides, and the chromatic response resembled the known pattern of iron deposition. More intense and extensive chromatic responses were noted in *Nrf2*-null mouse livers than in WT mouse livers, while deposition was poor in *Keap1*-kd mouse livers (Fig. 1a).

Journal : Large 535 | Dispatch : 9-2-2012 | Pages : 12
Article No. : 552 | LE | TYPESET
MS Code : JG-2011-11-OA-901 | CP | DISK

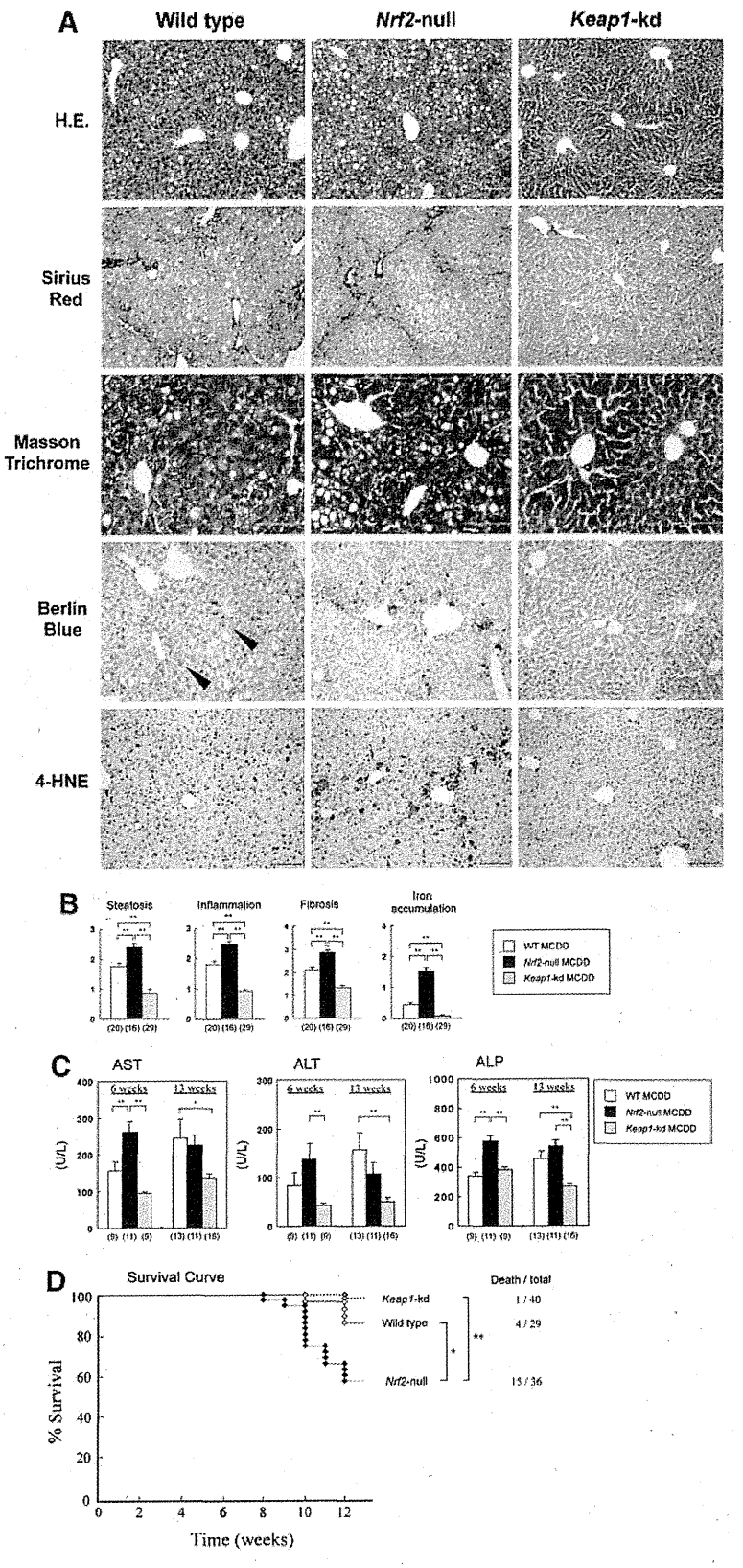

Fig. 1 Sustained activation of Nrf2 protects against progression of steatohepatitis induced by an MCDD. **a** H&E-, Sirius red-, Masson trichrome-, Berlin blue- and 4-HNE-stained sections of representative liver specimens from the WT, the *Nrf2*-null and *Keap1*-kd mice fed an MCDD for 13 weeks (bars 100 μm). **b** NAFLD activity score (NAS) in liver samples fed an MCDD for 13 weeks. Values are mean ± SE. $*P < 0.05$, $**P < 0.01$, significantly different between the two groups. The *numbers in parentheses* represent the number of animals examined in each group. **c** Analysis of blood biochemistry (AST, ALT and ALP) in the WT, *Nrf2*-null and *Keap1*-kd fed an MCDD for 6 or 13 weeks. The *numbers in parentheses* represent the number of animals examined in each group. **d** Survival curve in the WT, *Nrf2*-null and *Keap1*-kd mice

Journal : Large 535 | Dispatch : 9-2-2012 | Pages : 12
Article No. : 552 | LE | TYPESET
MS Code : JG-2011-11-OA-901 | CP | DISK

Pathological changes in the liver were quantified using the NAFLD activity score (NAS). The *Nrf2*-null mouse livers showed 1.5- to 2-fold greater changes in the scores for fat deposition, inflammation, fibrosis and iron deposition compared to the WT mouse livers, while these changes were approximately half as intense in the *Keap1*-kd mouse livers (Fig. 1b). Signs of steatohepatitis were more intense in the *Nrf2*-null mouse livers than in the WT mouse livers, while they were minimal in the *Keap1*-kd mouse livers, thus indicating that the activity of steatohepatitis is associated with the intensity of Nrf2 expression. Evaluation of hepatopathy on the basis of blood biochemical data showed that AST, ALT and ALP levels at 6 weeks after the start of MCDD treatment were higher in the *Nrf2*-null mouse than in WT and *Keap1*-kd mouse (Fig. 1c). At 13 weeks after beginning MCDD treatment, AST and ALT levels were higher in the WT mice than in the other mice, and elevated AST and ALT levels were suppressed in the *Keap1*-kd mice (Fig. 1c). This result may be attributable to a difference in the timing of the peak in hepatic dysfunction—peak of dysfunction in the WT mouse livers occurred later than that in the *Nrf2*-null mouse livers. The ALP level was significantly lower in *Keap1*-kd mice than in WT and *Nrf2*-null mice. Figure 1d shows the mouse survival curve. Death of *Nrf2*-null mice began 8 weeks after the start of MCDD treatment. By the end of the 13-week MCDD treatment, 15 of 36 *Nrf2*-null mice had died. Only a few WT and *Keap1*-kd mice had died. These results indicate that deletion of Nrf2 is fatal during prolonged MCDD treatment.

Suppression of hepatic fat accumulation and oxidative stress by Nrf2

Neutral fat levels in the liver tissue after 6-week control diet ingestion were significantly higher in *Nrf2*-null mice than in WT mice. Neutral fat levels in the *Keap1*-kd mouse livers were significantly lower than those in the WT mouse livers at both 6 and 13 weeks after the start of control diet ingestion (Fig. 2a). Six-week MCDD treatment resulted in significantly elevated neutral fat levels in WT and *Nrf2*-null mouse livers, while levels in *Keap1*-kd mouse livers were not elevated; neutral fat levels were significantly lower in *Keap1*-kd mouse livers than in WT and *Nrf2*-null mouse livers (Fig. 2a). Treatment with MCDD for 13 weeks resulted in elevated neutral fat levels in the *Keap1*-kd mouse liver, but similar to those with 6-week MCDD treatment. These levels remained significantly lower than in WT and *Nrf2*-null mouse livers (Fig. 2a).

We measured the levels of MDA, a lipid peroxide, to evaluate the intensity of oxidative stress in the liver tissue (Fig. 2a). Treatment with MCDD resulted in significantly

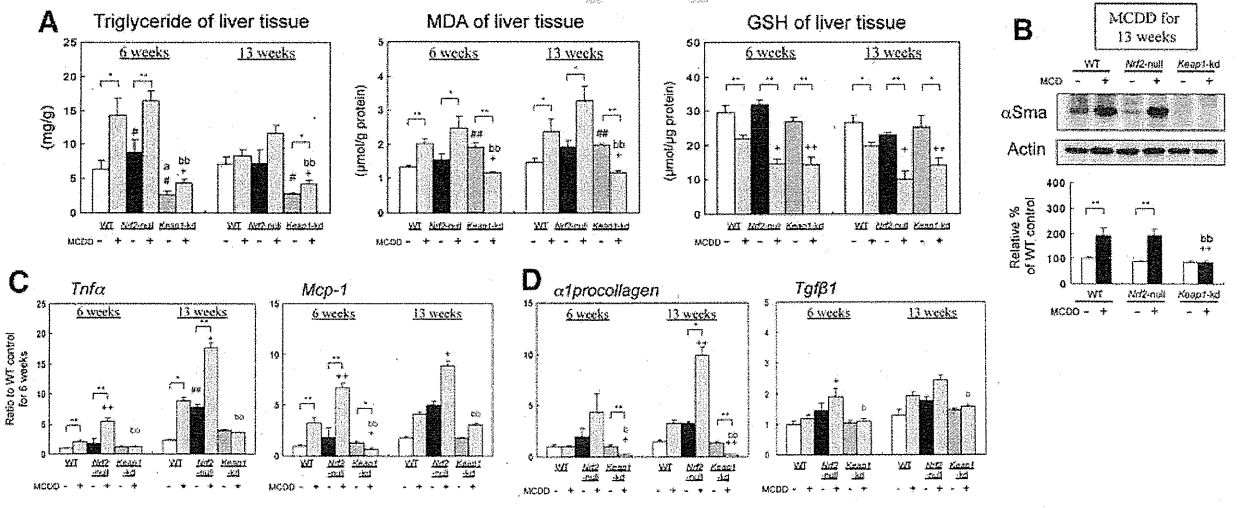

Fig. 2 Sustained activation of Nrf2 inhibits hepatic oxidative stress, inflammatory cytokines and fibrosis stimulation factors in steatohepatitis induced by an MCDD. **a** Triglyceride, malondialdehyde (MDA) and glutathione (GSH) of liver tissue in the WT, *Nrf2*-null and *Keap1*-kd mice fed an MCDD for 6 or 13 weeks. Data are given as mean ± SE (n = 8–15/group). $^{\#}P < 0.05$, $^{\#\#}P < 0.01$, significantly different from the WT with control feeding; $^{a}P < 0.05$, $^{aa}P < 0.01$, significantly different from the *Nrf2*-null with control feeding; $^{\dagger}P < 0.05$, $^{++}P < 0.01$, significantly different from the WT with MCD feeding; $^{b}P < 0.05$, $^{bb}P < 0.01$, significantly different from the *Nrf2*-null with MCD feeding; *brackets* $^{*}P < 0.05$, $^{**}P < 0.01$, significantly different between the two groups. **b** Immunoblot analysis of α-Sma proteins in livers of the WT, *Nrf2*-null and *Keap1*-kd fed a control diet or an MCDD for 13 weeks. *Bar graph* shows quantitation of optical density of the immunoblots. Data are given as mean ± SE (n = 8/group). **c** Steady-state mRNA levels of the factors involved in the inflammatory cytokines in livers of the WT, *Nrf2*-null and *Keap1*-kd mice fed a control diet or MCDD for 6 or 13 weeks. Data are given as mean ± SE (n = 6–7/group). **d** Steady-state mRNA levels of the factors involved in the fibrogenesis in livers of the WT, *Nrf2*-null and *Keap1*-kd mice fed a control diet or MCDD for 6 or 13 weeks. Data are given as mean ± SE (n = 6–7/group)

Journal : Large 535 | Dispatch : 9-2-2012 | Pages : 12
Article No. : 552 | LE | TYPESET
MS Code : JG-2011-11-OA-901 | CP | DISK

elevated MDA levels in WT and *Nrf2*-null mouse livers. MDA levels in *Keap1-kd* mouse livers were unexpectedly slightly higher than those in WT mouse livers at both 6 and 13 weeks after the start of control diet ingestion (Fig. 2a). Following MCDD treatment, MDA levels remained significantly lower in *Keap1*-kd mouse livers than in WT and *Nrf2*-null mouse livers (Fig. 2a).

Basal levels of GSH, an endogenous antioxidant found in the liver tissue, did not differ significantly among the WT, *Nrf2*-null and *Keap1*-kd mouse livers (Fig. 2a). At 6 and 13 weeks after the start of MCDD treatment, GSH levels were significantly lower than the pretreatment levels in WT, *Nrf2*-null and *Keap1*-kd mouse livers. Furthermore, the GSH level was significantly lower in *Nrf2*-null and *Keap1*-kd mouse livers than in the WT mouse livers. There was no significant difference in this parameter between *Nrf2*-null and *Keap1*-kd mouse livers.

Figure 2b shows the results of immunoblot analysis of the alpha smooth muscle actin (α-Sma) protein expression level, an indicator of HSC activation and hepatic fibrosis. At 13 weeks after the start of control diet ingestion, the α-Sma expression level did not differ among WT, *Nrf2*-null and *Keap1*-kd mouse livers, while treatment with MCDD increased the expression of α-Sma in WT and *Nrf2*-null mouse livers. No increase was observed in the *Keap1*-kd mouse livers; the level was significantly lower than that in WT and *Nrf2*-null mouse livers (Fig. 2b).

Quantitative PCR was used to analyze hepatic expression of *Tnf-α* and *Mcp-1* (inflammatory cytokines, Fig. 2c) and *α1-procollagen* and *Tgf-β1* (fibrosis stimulation factors, Fig. 2d). At 13 weeks after the start of control diet ingestion, *Tnf-α* expression was significantly higher in *Nrf2*-null mouse livers than in WT mouse livers. At 6 and 13 weeks after the start of MCDD treatment, *Tnf-α* expression was significantly higher than its pretreatment level in both WT and *Nrf2*-null mouse livers, with the magnitude of increase significantly greater in the *Nrf2*-null mouse livers than in the WT mouse livers. In the *Keap1*-kd mouse livers, *Tnf-α* expression did not increase and was significantly lower than that in WT and *Nrf2*-null mouse livers. Changes similar to those in *Tnf-α* expression in the liver were noted in the expression of *Mcp-1*, *α1-procollagen* and *Tgf-β1*. Expression levels of these factors were significantly higher in MCDD-treated *Nrf2*-null mouse livers. These results appear to reflect the presence of inflammatory cell infiltration and fibrosis in the histopathologic findings (Fig. 1a).

Changes in the expression of Nrf2 and antioxidative stress genes regulated by Nrf2

Immunoblot analysis was conducted to evaluate changes in the expression of Nrf2 and oxidative stress response genes regulated by Nrf2 following MCDD treatment. Following control diet ingestion, Nrf2 expression was not detected in the *Nrf2*-null mouse livers, while the *Keap1*-kd mouse livers showed approximately fourfold higher Nrf2 expression than the WT mouse livers, thereby indicating constitutive Nrf2 expression in the mouse livers (Fig. 3a). Nrf2 expression in the WT mouse livers was approximately threefold higher following 1-week MCDD treatment than following control diet ingestion. Interestingly, the increase in Nrf2 expression in the WT mouse livers attenuated over time and was not observed at 13 weeks after the start of MCDD treatment. In the *Keap1*-kd mouse livers, Nrf2 expression was high at baseline, and MCDD treatment did not induce a marked increase in Nrf2 expression. However, the *Keap1*-kd mouse livers showed a greater increase in Nrf2 expression following MCDD treatment than the WT mouse livers. This increase was also observed at 13 weeks after the start of MCDD treatment (Fig. 3a).

The expression levels of γ-glutamylcysteine synthetase γ-Gcs), a rate-limiting enzyme of GSH, NAD(P)H: quinone oxidoreductase 1 (Nqo1) and glutathione *S*-transferase a1 (Gsta1), which are detoxifying enzymes regulated by Nrf2, were low in *Nrf2*-null mouse livers and markedly high in *Keap1*-kd mouse livers following control diet ingestion, and this trend was similar to that of Nrf2 expression (Fig. 3b). Following treatment with MCDD, WT mouse livers showed an increase in the expression levels of γ-GCS, Nqo1 and Gsta1, and these increases were similar but slower than the increase in Nrf2 expression; their expressions were minimal or did not occur in *Nrf2*-null mouse livers. In *Keap1*-kd mouse livers, the basal expression level was high, and MCDD treatment did not markedly increase expression. However, Nqo1, Gsta1 and γ-Gcs expression levels following MCDD treatment were markedly higher in *Keap1*-kd mouse livers than in WT and *Nrf2*-null mouse livers.

Fig. 3 Immunoblot analysis of **a** Nrf2 proteins in nuclear fraction of livers and **b** Nqo1, Gsta1 and γ-Gcs proteins in livers of the WT, *Nrf2*-null and *Keap1*-kd mice fed a control diet or an MCDD for 1 or 6 or 13 weeks. *Bar graph* shows quantitation of optical density of the immunoblots. Data are given as mean ± SE ($n = 8$/group). $^{\#}P < 0.05$, $^{\#\#}P < 0.01$, significantly different from the WT with control feeding; $^{a}P < 0.05$, $^{aa}P < 0.01$, significantly different from the *Nrf2*-null with control feeding; $^{\dagger}P < 0.05$, $^{++}P < 0.01$, significantly different from the WT with MCD feeding; $^{b}P < 0.05$, $^{bb}P < 0.01$, significantly different from the *Nrf2*-null with MCD feeding; *brackets* $^{*}P < 0.05$, $^{**}P < 0.01$, significantly different between the two groups

Regulation of iron excretion from hepatocytes and suppression of liver tissue iron deposition by Nrf2

Histopathological examination showed that MCDD treatment resulted in a significant increase in iron deposition in

Journal : Large 535 | Dispatch : 9-2-2012 | Pages : 12
Article No. : 552 | LE | TYPESET
MS Code : JG-2011-11-OA-901 | CP | DISK

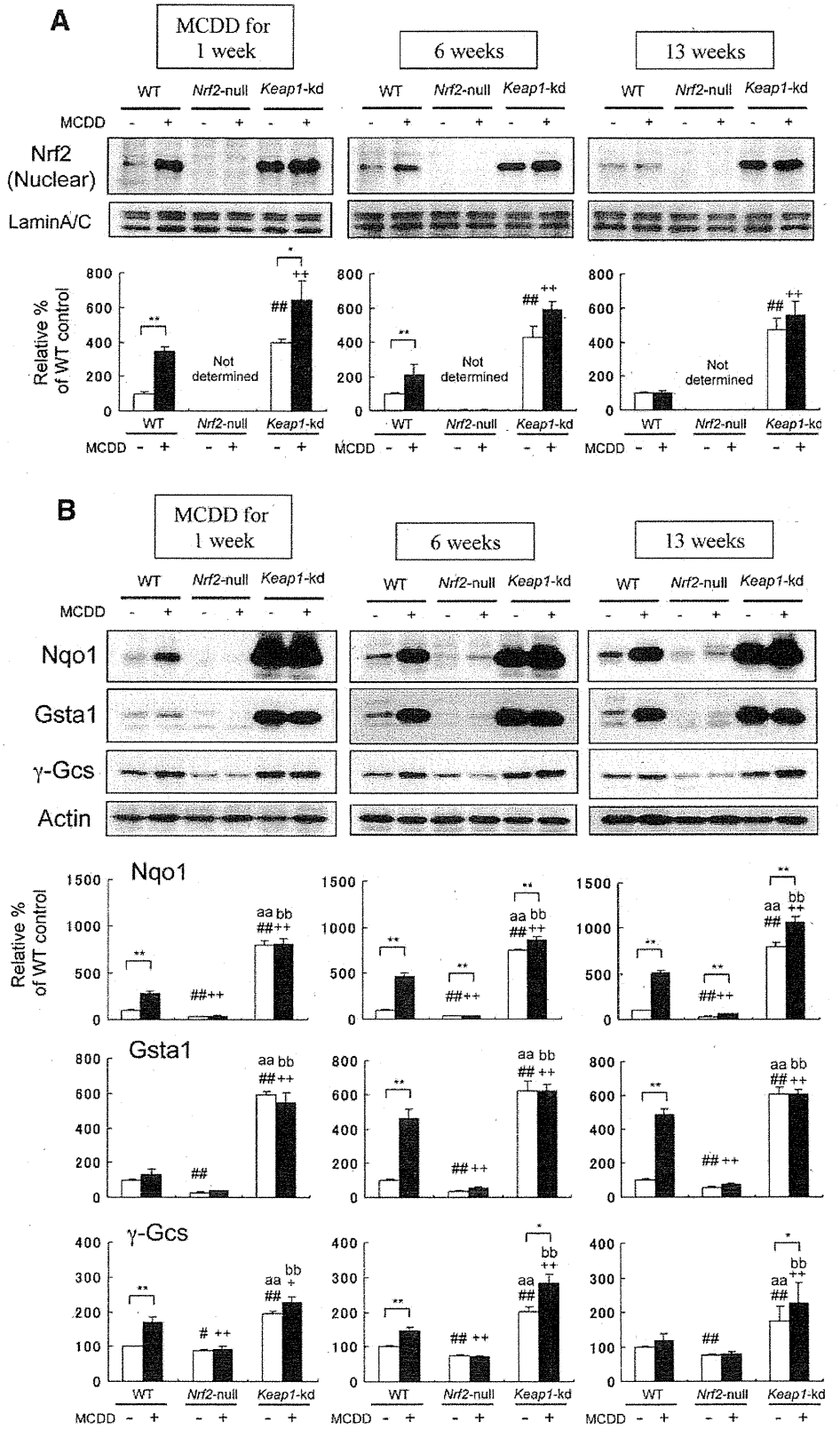

Journal : Large 535 Dispatch : 9-2-2012 Pages : 12
Article No. : 552 LE TYPESET
MS Code : JG-2011-11-OA-901 CP DISK